

A quad-port multiple-input-multiple-output system for underlay or interweave cognitive radio

Laith Wajeih Abdullah^{1,2}, Qasim Hadi Kareem³, Adheed Hasan Sallomi¹

¹Department of Electrical Engineering, College of Engineering, Mustansiriyah University, Baghdad, Iraq

²Communication Techniques Engineering Department, Technical Engineering College, Al-Furat Al-Awsat Technical University, Najaf, Iraq

³Computer Engineering Department, Al-Farabi University College, Baghdad, Iraq

Article Info

Article history:

Received Aug 18, 2022

Revised Nov 1, 2022

Accepted Nov 7, 2022

Keywords:

Cognitive radio

Multiple input multiple output

PIN diode

Reconfigurable antenna

Ultra-wideband

ABSTRACT

This paper presents a four-element frequency reconfigurable antenna system that is novel in terms of gathering both underlay and interweave cognitive radio in a single multiple input, multiple output (MIMO) design. Built on a 50×38×0.8 mm³ Rogers RT/Duroid 5880 substrate, this system is constructed of two scanning elements to sense ultra-wide band (UWB) with controllable band notching capabilities and two elements act as communication antennas. Eighteen MIMO modes can be provided depending on the state of the five positive-intrinsic-negative (PIN) diodes in each sensing antenna and the four PIN diodes in each communication antenna. These include a scanning UWB mode, fourteen modes to notch WiMax/Cband/wireless local area network (WLAN)/Xband/ITU in single/dual/triple/quad band rejection states and three interweave modes where each targeting one of the regions of WiMax/Cband/WLAN. Simulated by CST v.10; results like input reflection coefficient and realized gain verify system's capability to work in each operation mode. Moreover, mutual coupling, envelope correlation coefficient and diversity gain all evidence the performance of the proposed system as a MIMO system. Results, simple and compact profile, wide and flexible range of MIMO operation modes in line with the novelty to handle both underlay and interweave cognitive radio all nominate this system as promising to fulfill the needs of modern wireless communications.

This is an open access article under the [CC BY-SA](https://creativecommons.org/licenses/by-sa/4.0/) license.



Corresponding Author:

Laith Wajeih Abdullah

Communication Techniques Engineering Department, Technical Engineering College

Al-Furat Al-Awsat Technical University

Babylon-Najaf Street, Najaf 54003, Iraq

Email: coj.lat@atu.edu.iq

1. INTRODUCTION

Multiple input, multiple output (MIMO), the concept of having multiple antennas with duplicated functionality on the same substrate becomes day by day more essential to address the needs of the growing wireless communication world. Such antenna structures are indeed the corner stone in most fourth generation (4G) and fifth generation (5G) communication systems [1] mainly due to what they offer regarding high throughput and diversity merits [2]. MIMO, in conjugate with ultra-wide band (UWB) technology and its license-free utilization over the 3.1-10.6 GHz range approved by federal communications commission (FCC) in 2002, looks optimum to fulfill the high data rates needs of users in modern wireless communication [3]. However, what rises to disturb the UWB MIMO systems is having other wireless technologies that coexist in the UWB operation area of frequencies [4] and thus affect the quality of communications. Fortunately,

cognitive radio (CR), the technology presented by FCC as a methodology for better utilization of the available spectrum, and in its twofold; underlay and interweave [5], forms what looks so satisfactory solution for the previously mentioned problem. This, therefore, opened the way to have MIMO systems with UWB antennas based on CR that try to serve the demands of today and tomorrow in the wireless world.

Regarded underlay cognitive radio where bands in the interfered regions are to be excluded from the radiation, many MIMO designs have been reported. Khan *et al.* [6] presented 4-element MIMO system consists of UWB antennas with a reconfigurable structure in the ground plane to reject WLAN. In the 2-element MIMO design of [7], three positive-intrinsic-negative (PIN) diodes were used to configure its UWB antennas to reject WiMax/WLAN frequencies. Quddus *et al.* [8] suggested a MIMO system of two elements where a slot in each element's patch is controlled to exclude WLAN from system's UWB radiation.

On the other hand, many interweave CR designs have been reported where the MIMO system is capable to scan a wide band and configured to work within a specific region within this band. The 2×2 MIMO system of [9] has been suggested to scan the band (2.35-5.9 GHz) by two sensing antennas, while the other two antennas are tunable in the band (2.6-3.6 GHz) by varactor diodes. Zhao *et al.* [10] presented a 2-element MIMO system where its antennas can be configured by PIN and varactor diodes either to scan the wide band (1-4.5 GHz) or to operate in narrow bands within the range (0.9-2.6 GHz). Finally, the system presented in [11] covers the band (0.75-7.65 GHz) by the monopole scanning antenna while MIMO functionality in communication process can be achieved by two slot antenna that are tunable in the range (1.75-2.48 GHz).

In this paper, a 2×2 antenna system is presented as CR MIMO design which is to the best of our knowledge can be considered novel due its capability to gather underlay and interweave CR on one platform. Four frequency reconfigurable antennas, two as UWB antennas with on-demand band notching and two for communication purposes, are used to obtain the multi-functionality of the proposed system. Reconfiguration to desired mode of operation is achieved by the proper configuration of the eighteen PIN diodes distributed among the four antennas of this design. This configuration provides eighteen MIMO modes; one for UWB sensing, fourteen underly modes to notch one or more of WiMax/Cband/wireless local area network (WLAN)/Xband/ITU regions, and three interweave modes targeting one of the WiMax/Cband/WLAN regions. This $50 \times 38 \times 0.8$ mm³ MIMO system exhibits high flexibility to ban or operate in specific bands. This when conjugated with the results regarding its functionality on individual element basis or as a MIMO system, all make this system feasible to serve the demands of new wireless technologies.

2. ANTENNA SYSTEM DESIGN

The four-element CR system of this work is built on the two sides of a 0.8 mm Rogers RT/Duroid 5880 substrate with 2.2 dielectric constant and 0.0009 tangential loss. Two of the four antennas of this design are UWB antennas with on-demand band rejection capability, while the rest are frequency reconfigurable communication antennas. In the 50×38 mm² substrate used as the base of this quad antenna system, each UWB antenna occupies a 22×23 mm² area, while a 11.5×25 mm² space is required for each communication antenna. Figure 1 describes the layout and geometry of the proposed design, where the front and rear views are displayed in Figure 1(a) and Figure 1(b) respectively. Optimized values (in mm) of the parameters of this Figure 1 are:

Substrate: L=50, W=38 ; Ant#1: LA=22, WA=23, a1=1.5, a2=0.75, a3=2, a4=2.5, a5=6.3, a6=1.6, a7=0.8, a8=1.75, a9=0.9, a10=1.1, a11=5, a12=5, a13=0.7, a14=0.2, a15=0.2, a16=0.2, a17=2, a18=14, a19=5.5, a20=1.15, a21=0.2, a22=1.75, a23=0.5, ra1=0.45, ra2=0.7, ra3=0.7, ra4=0.45, ra5=0.7, ra6=0.5, ra7=1.9, ra8=1.2, ra9=4, ra10=2, ra11=3.5, ra12=0.45, ra13=4, ra14=9.5, ra15=0.5, ra16=9.5, ra17=0.4; Ant#3: LB=11.5, WB=25, b1=1.5, b2=0.75, b3=2.5, b4=2.75, b5=7, b6=0.75, b7=1.5, b8=1.75, b9=2, b10=7, b11=3.5, b12=1.75, b13=0.5, rb1=0.7, rb2=1.5, rb3=1, rb4=4, rb5=0.25, rb6=3.8, rb7=0.5, rb8=10, rb9=1, rb10=8, rb11=0.5.

Construction procedure of this MIMO antenna system is started by building the UWB antenna. This step is followed by modifying this antenna to have frequency notching behavior. Next, is to design the second antenna which is responsible for communication in specific ranges within the UWB spectrum. The fourth step is to build the MIMO antenna system from the predesigned single elements. Finally, this system is controlled by switching elements that are set to achieve MIMO operation as an underlay/interweave CR system.

2.1. UWB antenna

The UWB antenna is the first element to be built in this MIMO system. This antenna which is essential in scanning process of underlay/interweave modes of this CR system is based on a wide slot antenna with a rectangular radiating stub. The UWB antenna of this design -named Ant#1- is subjected to many modifications to improve its operation over the 3.1-10.6 GHz range. The main modifications with their impact on its input reflection coefficient are shown in Figure 2.

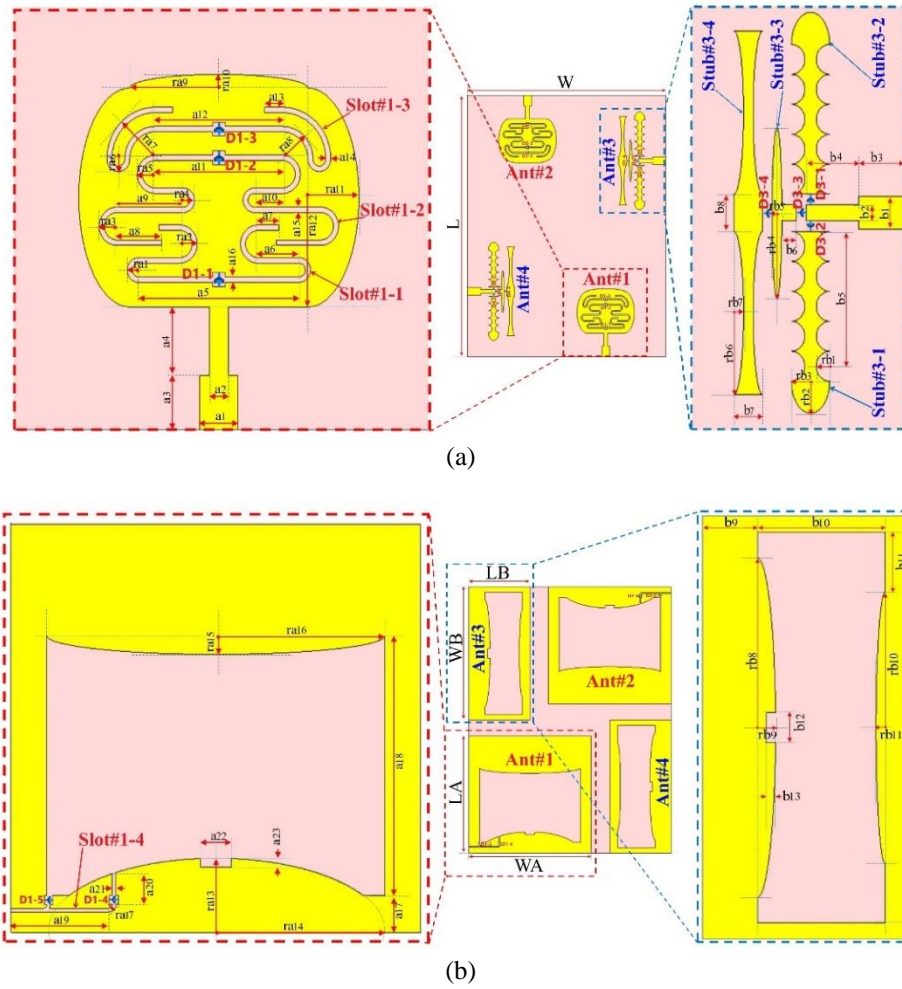


Figure 1. MIMO system geometry (a) front view and (b) rear view

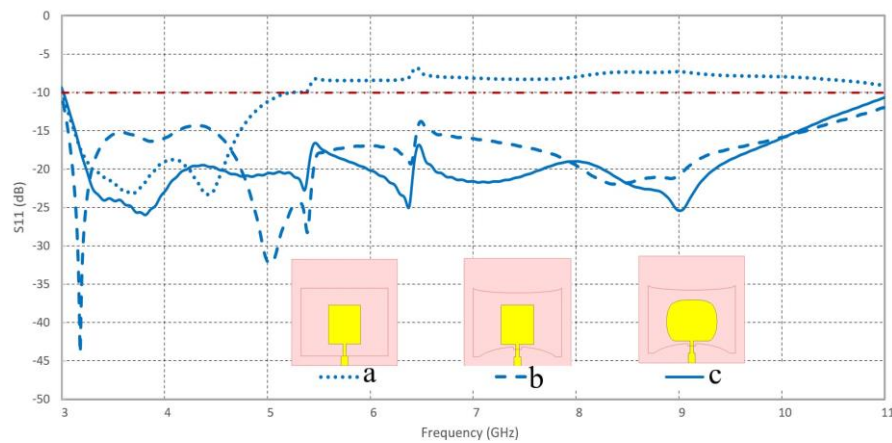


Figure 2. Modifications on Ant#1 and their impact on S11

2.2. Band rejection

In the underlay operation modes, the UWB antenna should have the ability to avoid radiation in the undesired regions of the spectrum. In our design, this goal was achieved by engraving three slots in the patch of the UWB antenna and one slot into its back plane as shown in Figure 1. The slots of the front plane are

formed as meandered line slots that overlap and distributed symmetrically along the longitudinal axis of the patch. The creation of these slots -named Slot#1-1, Slot#1-2 and Slot#1-3- to exclude ITU, WLAN and Xband is done in a successive manner. These slots are created as $\lambda_g/2$ slots where their lengths can be approximated depending (1) to (3) [12], [13]:

$$L_{slot} \approx \frac{\lambda_g}{2} \tag{1}$$

$$\lambda_g = \frac{c}{f_{notch} \sqrt{\epsilon_{eff}}} \tag{2}$$

$$\epsilon_{eff} \approx \frac{\epsilon_r + 1}{2} \tag{3}$$

where: L_{slot} : slot length, f_{notch} : notched frequency, λ_g : guided wavelength, c : velocity of light, ϵ_{eff} : effective dielectric constant and ϵ_r : relative dielectric constant.

On the back side of the antenna, an f-shape slot is to be created in the lower corner of the ground plane. Creation of this slot -named Slot#1-4- results in the exclusion WiMax and Cband from the UWB radiation. Figure 3 shows how optimization of slots' parameters affects the S11 response of the antenna to reject the targeted bands. This effect on rejection of the bands of ITU, WLAN, Xband and WiMax+Cband is displayed in Figures 3(a), 3(b), 3(c) and 3(d) respectively.

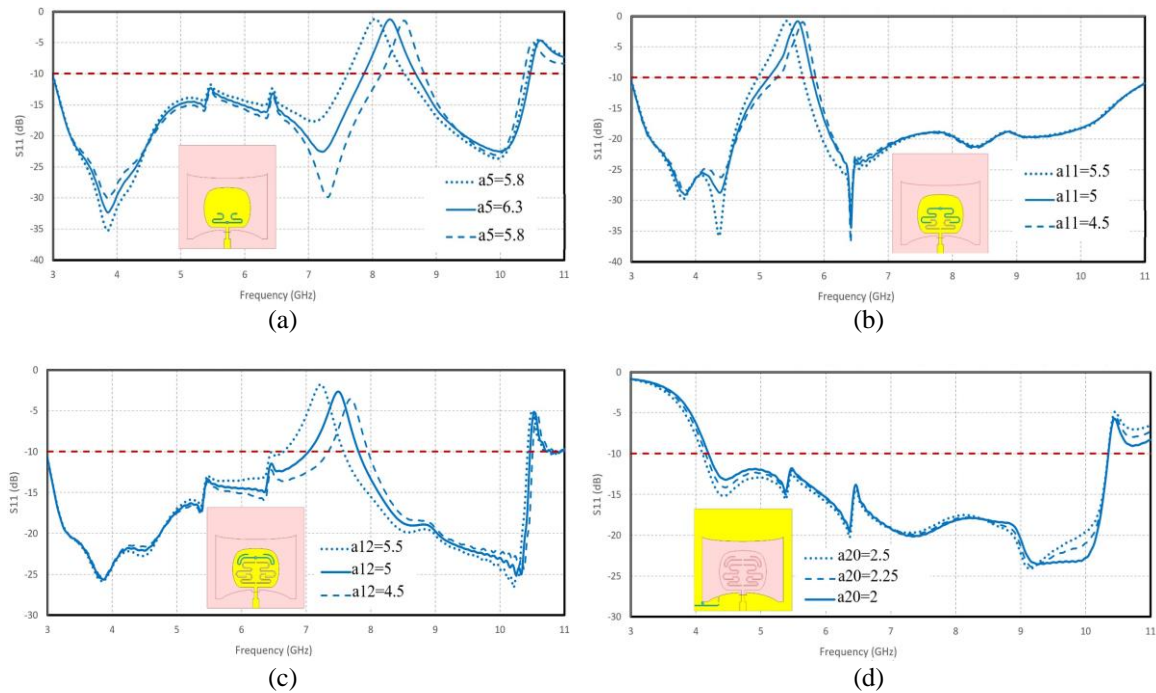


Figure 3. Parametric effect on input reflection coefficient of Ant#1 rejecting (a) ITU, (b) WLAN, (c) Xband, and (d) WiMax and Cband

2.3. Communication antenna

In this design, the function of radiation in only specific bands within the UWB range is achieved by a separate communication antenna. The radiator of this antenna-named Ant#3- basically consists of four stubs named Stub#3-1, Stub#3-2, Stub#3-3 and Stub#3-4. These stubs that are built in a consecutive manner brings the operation of the antenna to the desired region upon the connection/disconnection of the proper stub(s) to/from the feed of antenna. To work in Cband region, a symmetric pair of modified line stubs (Stub#4-1 and Stub#4-2) are connected to feedline to form a T-Shape radiator. This pair of stubs must be split from the feed in the rest communication modes targeting WiMax and WLAN In WiMax operation, Stub#3-3 with its modified T-shape is connected to feedline, while radiation in the WLAN is achieved by the cascaded attachment of both Stub#3-4 and Stub#3-3 to the feedline. Optimization of parameters regarding these stubs

affects the response of Ant#3 as shown in Figure 4, and examples on this impact on the input reflection coefficient in communication within the targeted bands are displayed in Figures 4(a)-4(c).

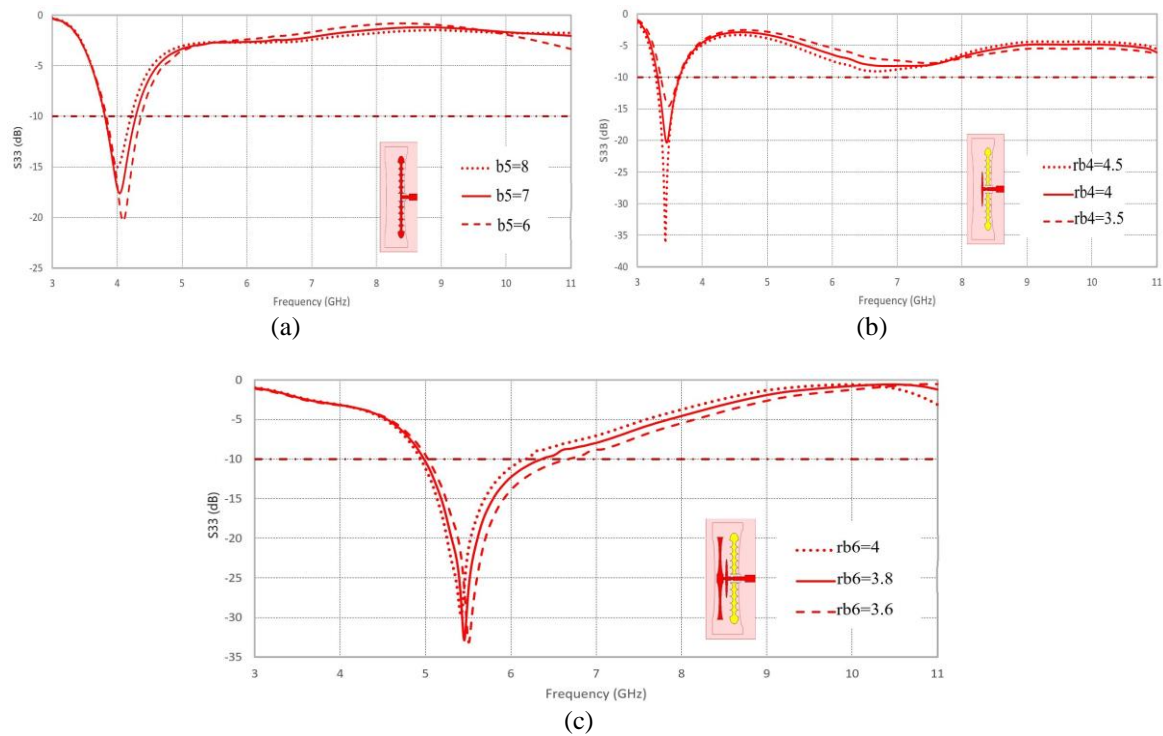


Figure 4. Parametric effect on input reflection coefficient of Ant#3 at (a) Cband, (b) WiMax, and (c) WLAN

2.4. MIMO antenna system

The UWB/communication antennas of the previous sections are duplicated by another two antennas -named Ant#2 and Ant#4- to form the 4-elment MIMO system. The UWB antennas are placed on opposite corners of the substrate while the other two corners are used for the communication antenna pair. Moreover, feed layouts of the two sets of antennas are made orthogonal to each other. This arrangement of the two sets of antennas has a significant effect to reduce mutual coupling.

2.5. Configuration

To have UWB operation, on-demand band rejection and multi band communication; the proposed antenna system has to be reconfigurable. Reconfigurability in this MIMO is achieved by nine pairs of HPND-4005 PIN diodes as illustrated in Figure 1. The on/off configuration of these diodes affects the operation of the antenna by enabling/disabling specific slots in the UWB set of antennas or specific radiating stubs in the communication set of antennas. Figure 5 shows the the equivalent circuits of the 4005-HPND PIN diode, where these circuits of the ON and OFF states of the diode are shown in Figure 5(a) and Figure 5(b) respectively [14], [15]. Useable configuration states of the PIN diodes of the proposed work along with the details of related operation modes are tabulated in Table 1.



Figure 5. Equivalent circuit of HPND-4005 PIN diode at (a) ON-state and (b) OFF-state

Table 1. Operation modes

Mode	D1-1,	D1-2,	D1-3,	D1-4,	D1-5,	D3-1,	D3-2,	D3-3,	D3-4,	Cognitive Radio	Function	Targeted bands
	D2-1	D2-2	D2-3	D2-4	D2-5	D4-1	D4-2	D4-3	D4-4			
MU#0	1	1	0	0	0	0	0	0	0	Underlay	Scanning	UWB
MU#1.1	0	1	1	1	1	0	0	0	0	Underlay	Single band rejection	ITU
MU#1.2	1	0	1	1	1	0	0	0	0			WLAN
MU#1.3	1	1	0	1	1	0	0	0	0			Xband
MU#1.4	1	1	1	0	1	0	0	0	0			WiMax
MU#2.1	1	1	1	1	0	0	0	0	0	Underlay	Dual band rejection	WiMax+Cband
MU#2.2	0	1	0	1	1	0	0	0	0			Xband+ITU
MU#2.3	0	1	1	0	1	0	0	0	0			WiMax+ITU
MU#2.4	1	0	1	0	1	0	0	0	0			WiMax+WLAN
MU#2.5	1	1	0	0	1	0	0	0	0			WiMax+Xband
MU#3.1	1	0	0	0	1	0	0	0	0	Underlay	Triple band rejection	WiMax+WLAN+Xband
MU#3.2	0	1	1	1	0	0	0	0	0			WiMax+Cband+ITU
MU#3.3	1	0	1	1	0	0	0	0	0			WiMax+Cband+WLAN
MU#3.4	1	1	0	1	0	0	0	0	0			WiMax+Cband+Xband
MU#4	1	0	0	1	0	0	0	0	0	Underlay	Quad band rejection	WiMax+Cband+WLAN+Xband
MI#1.1	1	1	1	1	1	1	1	0	0	Interweave	Scanning+Comm.	UWB+Cband
MI#1.2	1	1	1	1	1	0	0	1	0			UWB+WiMax
MI#1.3	1	1	1	1	1	0	0	1	1			UWB+WLAN

3. RESULTS AND DISCUSSION

3.1. Input reflection coefficient

Input reflection coefficient results evidences the functionality of the antenna to meet the operation bandwidth. In our design, the results related this coefficient, S11 and S33 for Ant#1 and Ant#3 are presented in this section. Input reflection coefficient results of the design in the underlay modes are shown in Figure 6. Having all the switches of Ant#1 in the on position, it can be that S11 curves meet the -10 dB condition along the UWB range.as shown in Figure 6(a). In underlay modes, only Ant#1 is considered, thus all sections of Ant#3 are disabled. Here, the on/off configuration of the diodes disables/enables notching effect of the slots within the UWB antenna. S11 results of Figure 6(b) shows the notching effect to exclude ITU, WLAN, Xband and WiMax from the radiation of Ant#1 when disabling D1-1, D1-2, D1-3, and D1-4 respectively. Dual band notching is presented in the curves of Figure 6(c) as a result either to disable a pair of the diodes D1-1 to D1-4 of or disabling only D1-5. The value of S11 is above the -10 dB line for the three targeted bands in the modes of Figure 6(d) which ensures the capability of the system in triple band rejection. Finally, disabling D1-1, D1-2 and D1-4 results in the curve of Figure 6(e) where ITU, WLAN, WiMax and Cband regions are not included in the wide band radiation of Ant#1.

Input reflection coefficient results of the design in the interweave modes are shown in Figure 7. The condition of -10 dB is realized along the UWB frequencies for Ant#1 in the three modes of Figure 7(a). It can also be seen that S11 response differs slightly in the curves of Figure 7(a) when compared with Figure 6(a) due to the consideration of mutual coupling of other antennas in this MIMO design. On the other hand, in the interweave modes, Ant#3 response proves system's ability to handle communication in the targeted bands. This can be shown in of Figure 7(b) where S33 is below -10 dB for Cband, WiMax and WLAN in MI#1.1, MI1.2 and MI1.3 respectively.

3.2. Realized gain

Realized gain is another proof of the functionality of the antenna in scanning/band-notching phases of operation as displayed in Figure 8. For Ant#1, it can be shown that realized gain is positive and satisfactory along the 7.5 GHz of UWB range as illustrated in Figure 8(a). It can also be seen that this gain suffers sudden and sever degradation in the prohibited regions for the single band rejection modes of operation as presented in Figure 8(b). Two falls in realized gain value can also be noticed at the rejected bands in the curves of Figure 8(c). Realized gain also drops in the three banned regions of the plots regarding modes MU#3.1, MU#3.2, MU#3.3 and MU#3.4 of Figure 8(d). Finally, Figure 8(e) shows how realized gain decreases at WiMax, Cband, WLAN and Xband regions in MU#4.

Realized gain results for interweave operation are presented in Figure 9. It is seen that the realized gain results of Ant#1 displayed in Figure 8(a) in scanning process are nearly like that of Figure 9(a) but with only slight variations due to the effect of other antennas' radiation. It can also be observed that realized gain is almost greater than 3 dB along Cband, WiMax and WLAN regions for MI#1.1, MI#1.2 and MI#1.3 modes as illustrated in the results of Figure 9(b).

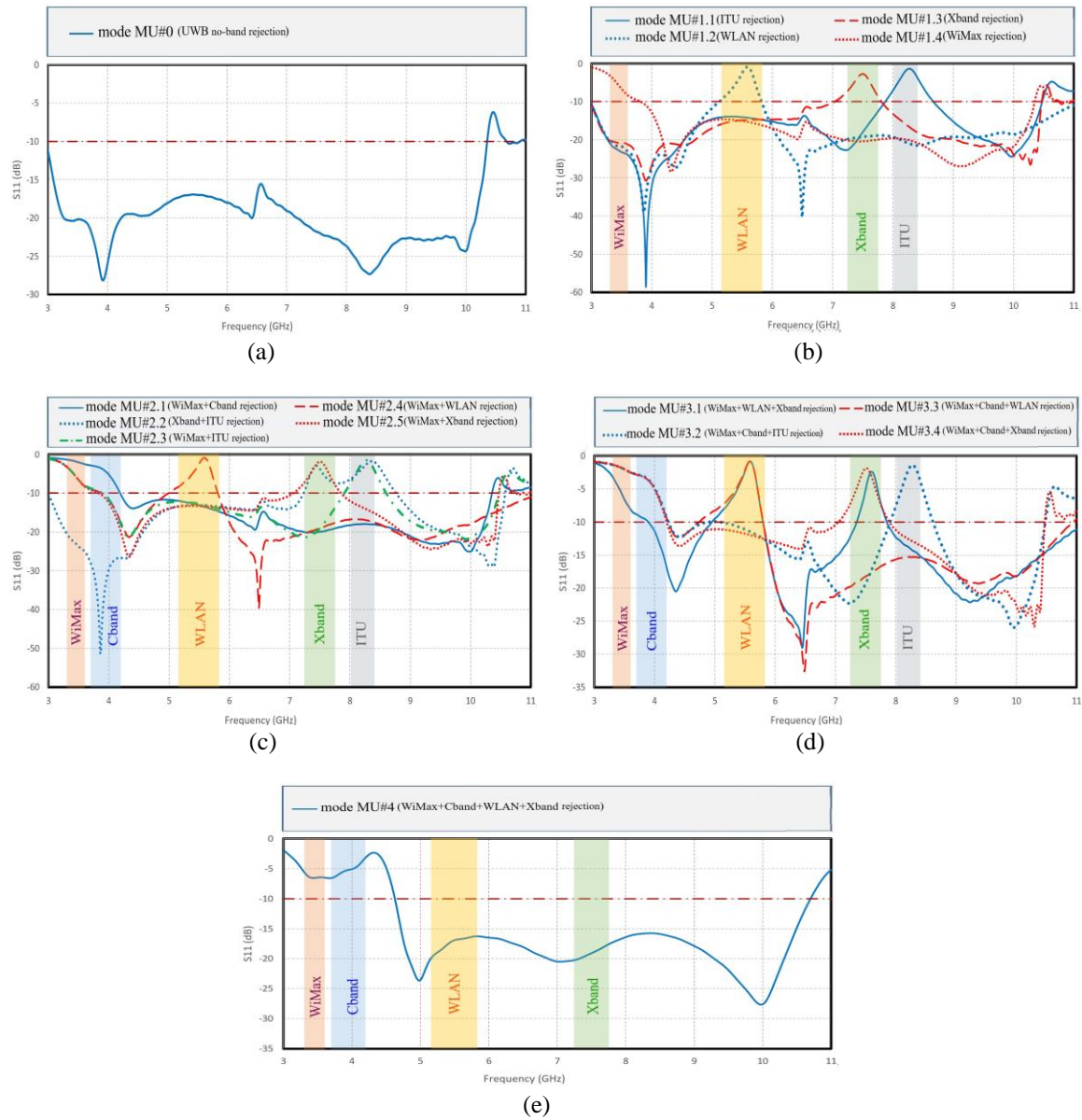


Figure 6. Input reflection coefficient of Ant#1 at (a) UWB mode, (b) single-band rejection modes, (c) dual-band rejection modes, (d) triple-band rejection modes, and (e) quad-band rejection mode

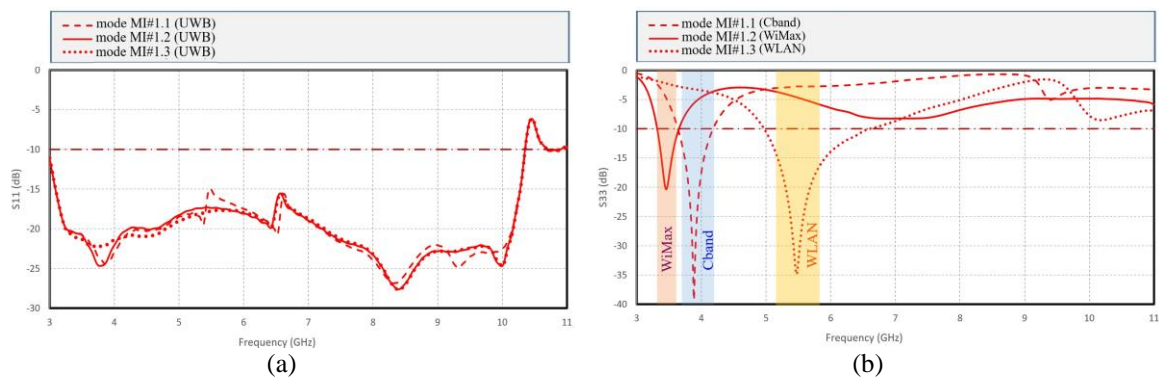


Figure 7. Input reflection coefficient of (a) Ant#1 in the interweave modes, and (b) Ant#3 in the interweave modes

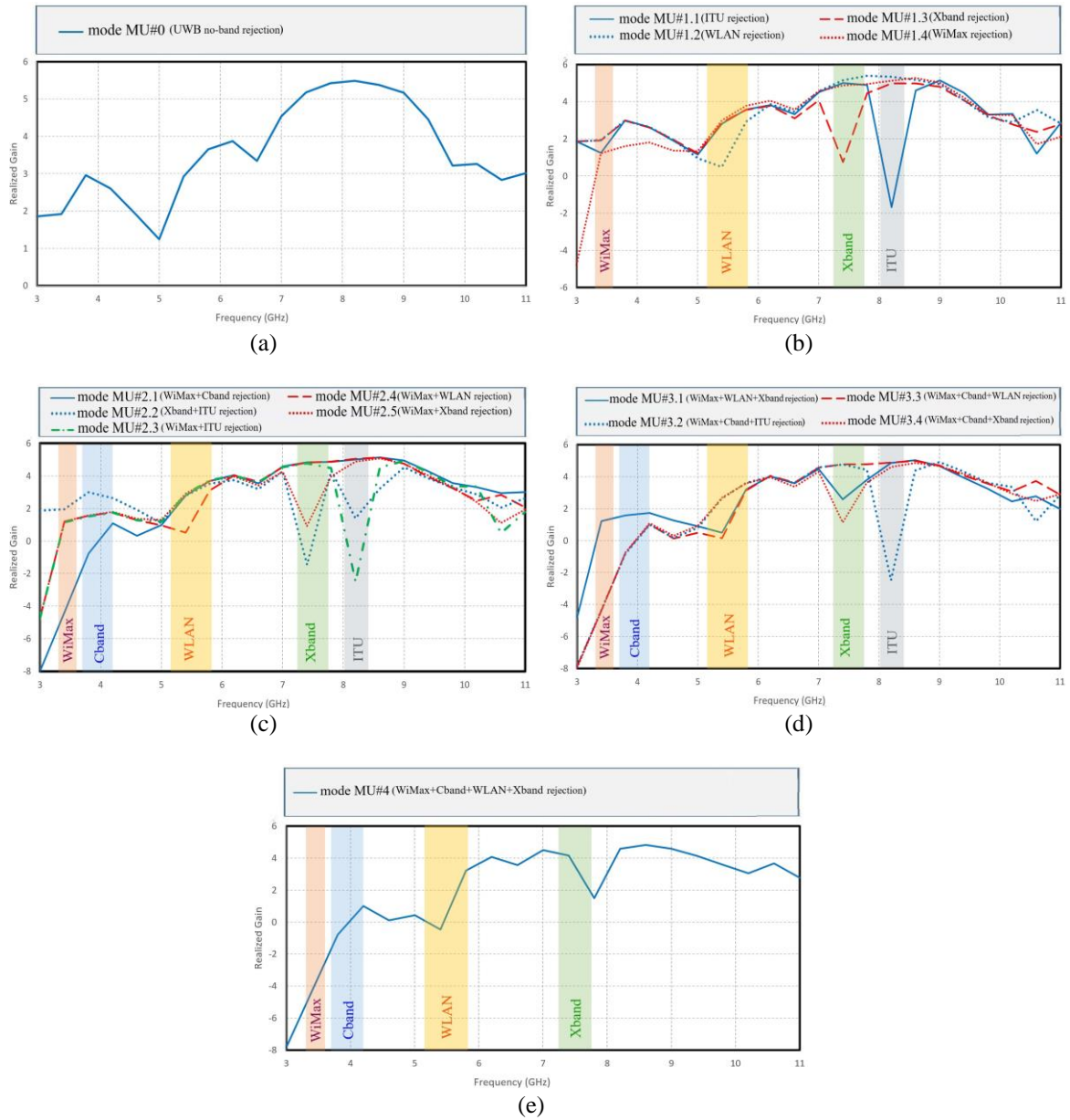


Figure 8. Realized gain of Ant#1 at (a) UWB mode, (b) single-band rejection modes, (c) dual-band rejection modes, (d) triple-band rejection modes, and (e) quad-band rejection mode

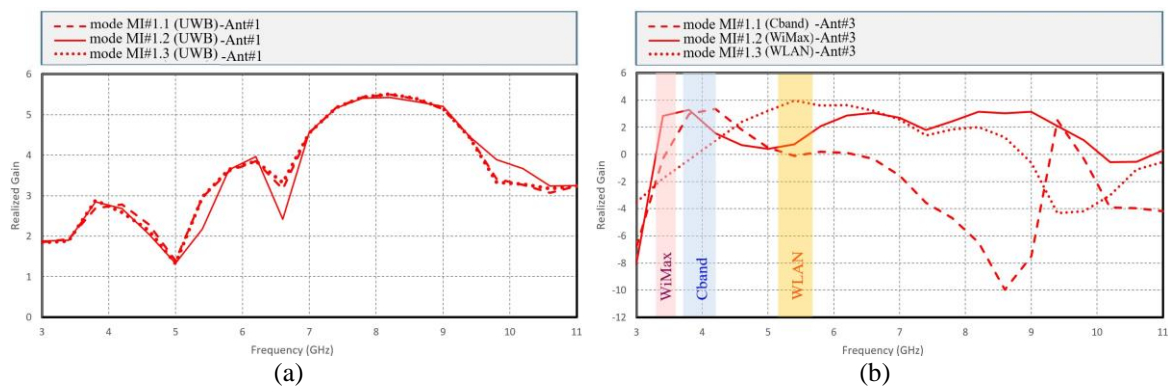


Figure 9. Realized gain of (a) Ant#1 in the interweave modes and (b) Ant#3 in the interweave modes

3.3. Surface current distribution

Behavior of the antenna to notch targeted bands can be better understood when observing how current is distributed in the band-rejection modes as shown in Figure 10. Here, it is noticeable that currents are circulating around the $\lambda/2$ slot which leads to ban a band centered at a frequency that is inversely related to twice of the length of the activated slot. Such current distributions around Slot#1, Slot#2 and Slot#3 that leads to prohibit ITU, WLAN and Xband are illustrated in Figures 10(a), 10(b) and 10(c) respectively.

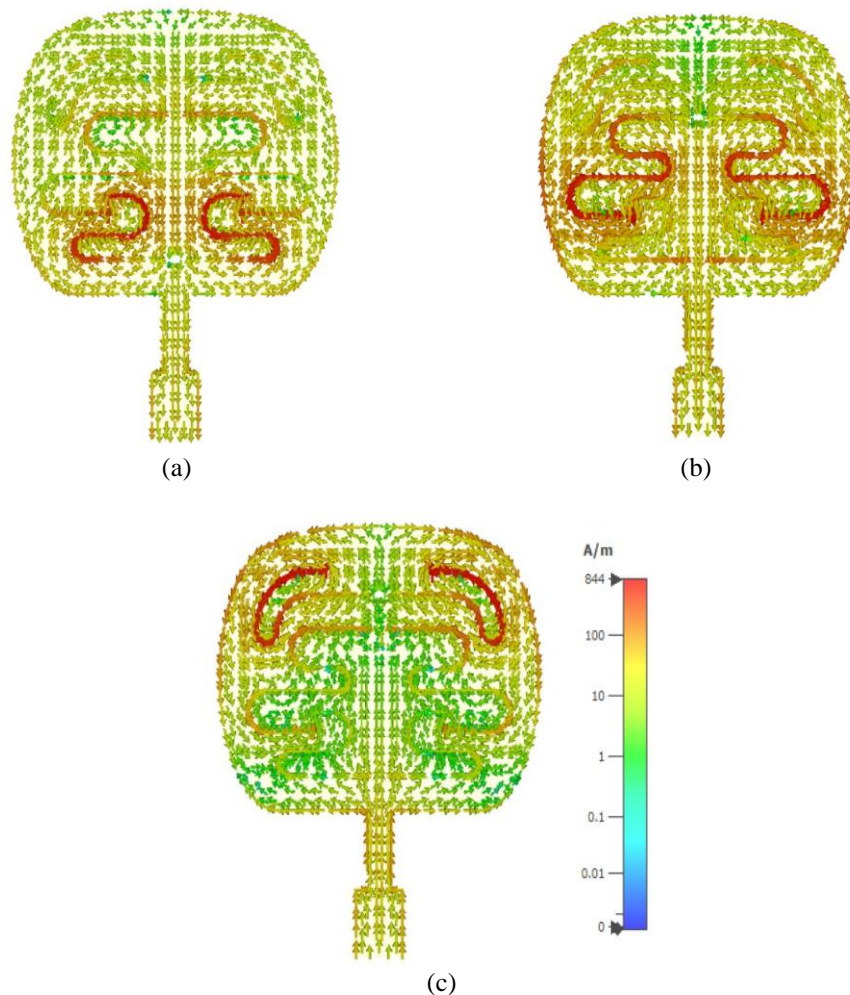


Figure 10. Surface current of Ant#1 in (a) mode MU#1.1 @ 8.3 GHz (b) mode MU#1.2 @ 5.6 GHz, and (c) mode MU#1.3 @ 7.5 GHz

3.4. Mutual coupling

Mutual coupling is so important to assess the performance of multi-antenna systems. It draws an image of the interaction between the antennas of the MIMO system which is usually desired to be as small as possible. Mutual coupling in the underlay modes of operation is shown in Figure 11. Despite that a 15 dB isolation is considered acceptable in MIMO designs [16], coupling between the scanning antennas in this design is almost kept below -20 dB between the UWB antennas along the 3.1-10.6 GHz range whether in UWB mode of Figure 11(a) or the band rejection modes of Figures 11(b) to 11(e).

Figure 12 displays mutual coupling in the interweave operation modes. In Figure 12(a) which describes isolation between Ant#1 and Ant#2 in scanning process of the interweave modes, S_{12} results are somehow like those of Figure 11(a) with small distinctions due to interaction with the communication antennas of this MIMO system. On the other hand, how communication antennas are isolated from the UWB antenna is described in Figure 12(b) and Figure 12(c) where S_{13} and S_{14} are under the -15 dB margin. Finally, it can be shown that good isolation is obtained between communication antennas where S_{34} results of Figure 12(d) are almost below -20 dB for the three interweave modes.

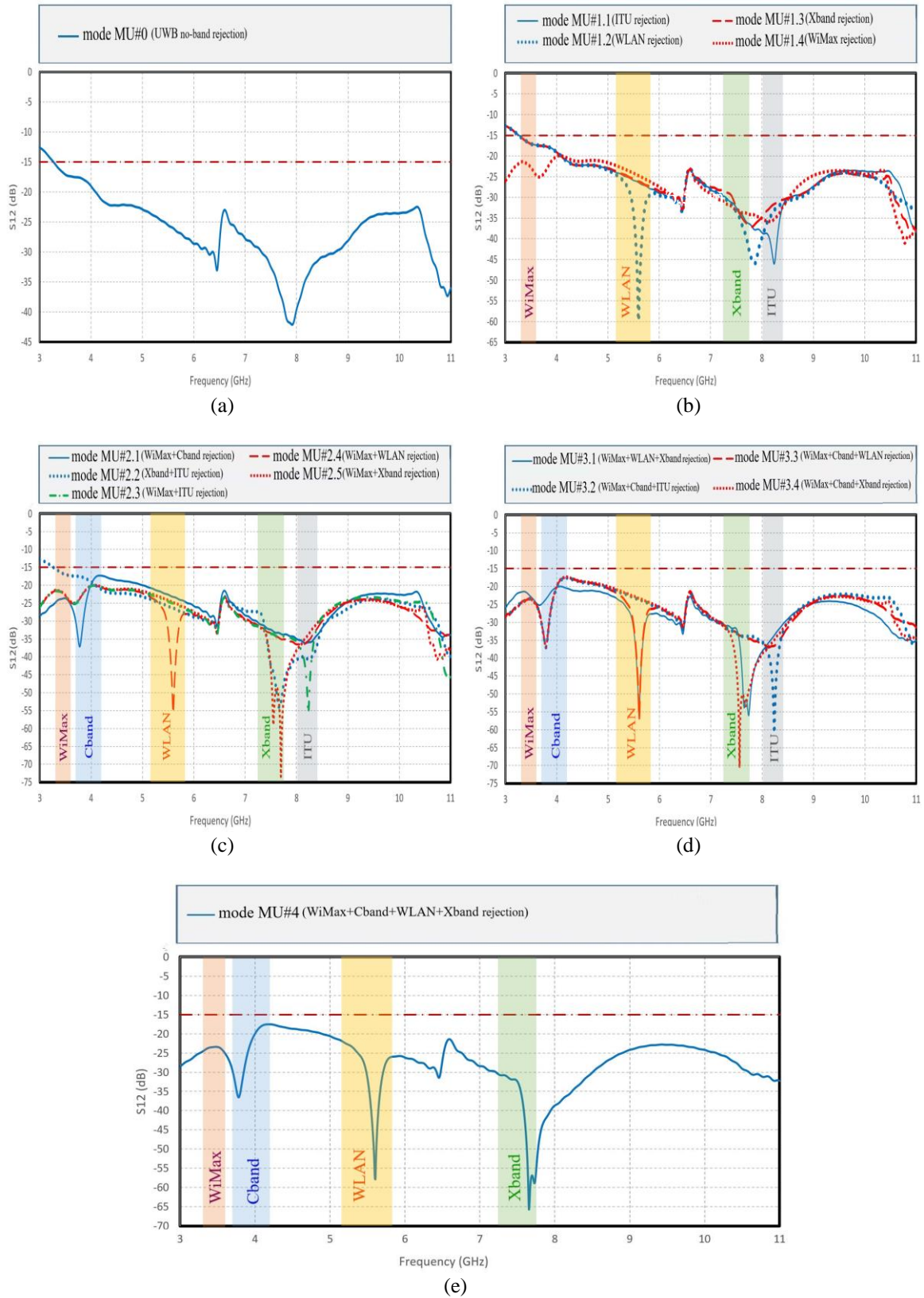


Figure 11. Mutual coupling between Ant#1 and Ant#2 at (a) UWB mode, (b) single-band rejection modes, (c) dual-band rejection modes, (d) triple-band rejection modes, and (e) quad-band rejection mode

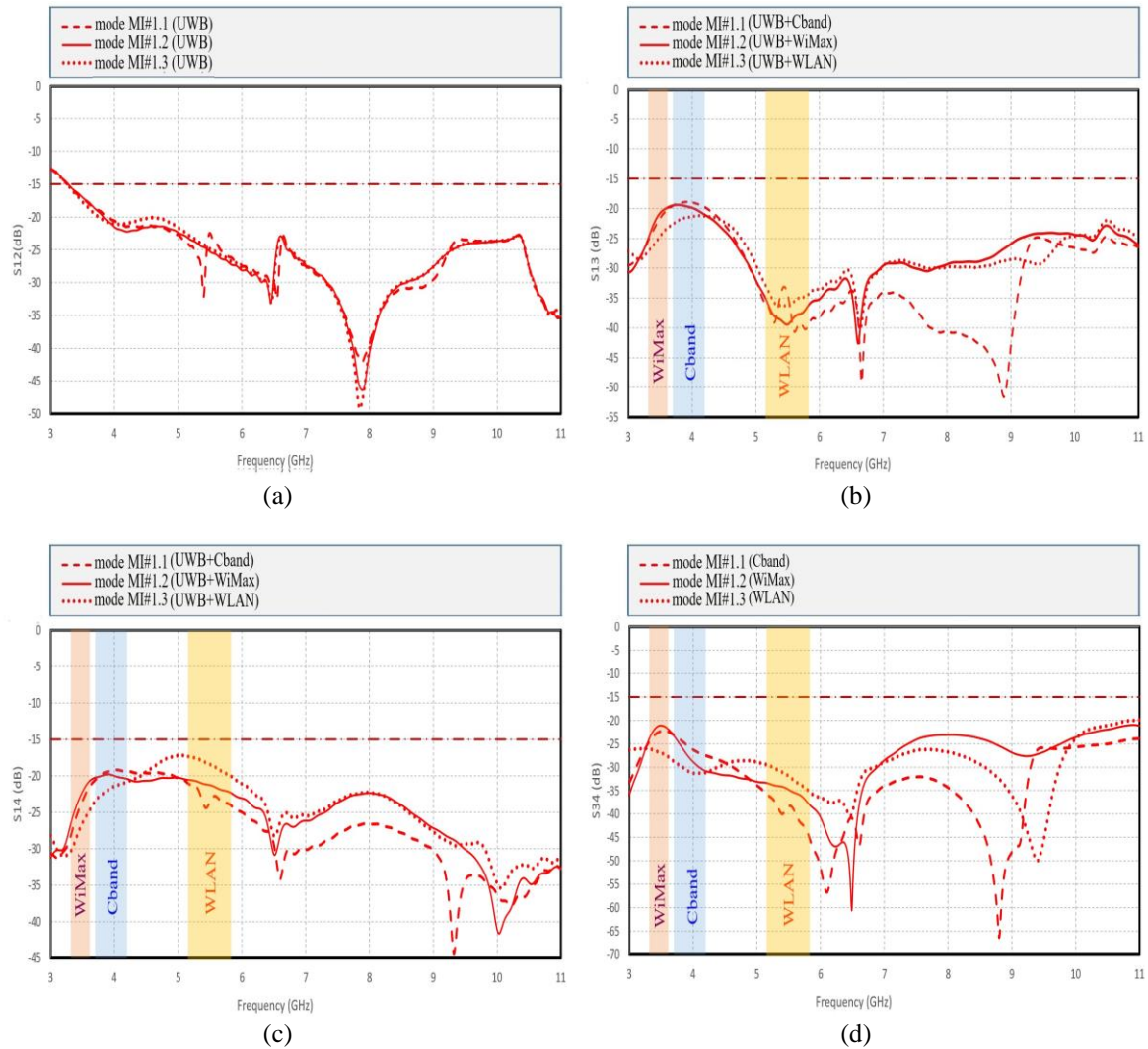


Figure 12. Mutual coupling in interweave modes between (a) Ant#1 and Ant#2, (b) Ant#1 and Ant#3, (c) Ant#1 and Ant#4, and (d) Ant#3 and Ant#4

3.5. Envelope correlation coefficient

Envelope correlation coefficient (ECC) is used in MIMO terminology as an indicator of the good isolation between the elements composing the multi-antenna system. ECC -expressed by ρ_e - can be calculated from S-parameters of the MIMO system as described in (4) [17], [18].

$$\rho_e = \left| \frac{|s_{ii}^* s_{ij} + s_{ji}^* s_{jj}|}{\sqrt{(1-|s_{ii}|^2 - |s_{ji}|^2)(1-|s_{jj}|^2 - |s_{ji}|^2)}} \right|^2 \tag{4}$$

ECC should be lower than 0.5 in feasible MIMO designs [19]. This section presents ECC values in all operation modes for the proposed antenna system. As it can be seen, these values are far below the 0.5 condition in all cases of Figure 13 and Figure 14 which ensures well separation between the four elements of this design. Figure 13(a) shows that ECC is approaching zero along the UWB range in sensing mode. It is also obvious that ECC is lower than 0.15 along the 3.1-10.6 GHz range in band rejection modes shown in Figures 13(b) to 13(e). Furthermore, Figure 14(a) proves good isolation between sensing antennas by ECC values close to zero in three interweave modes. At the end, good isolation is guaranteed in this MIMO design between communication antennas where ECC doesn't exceed 0.005 in the operation regions of Figure 14(b).

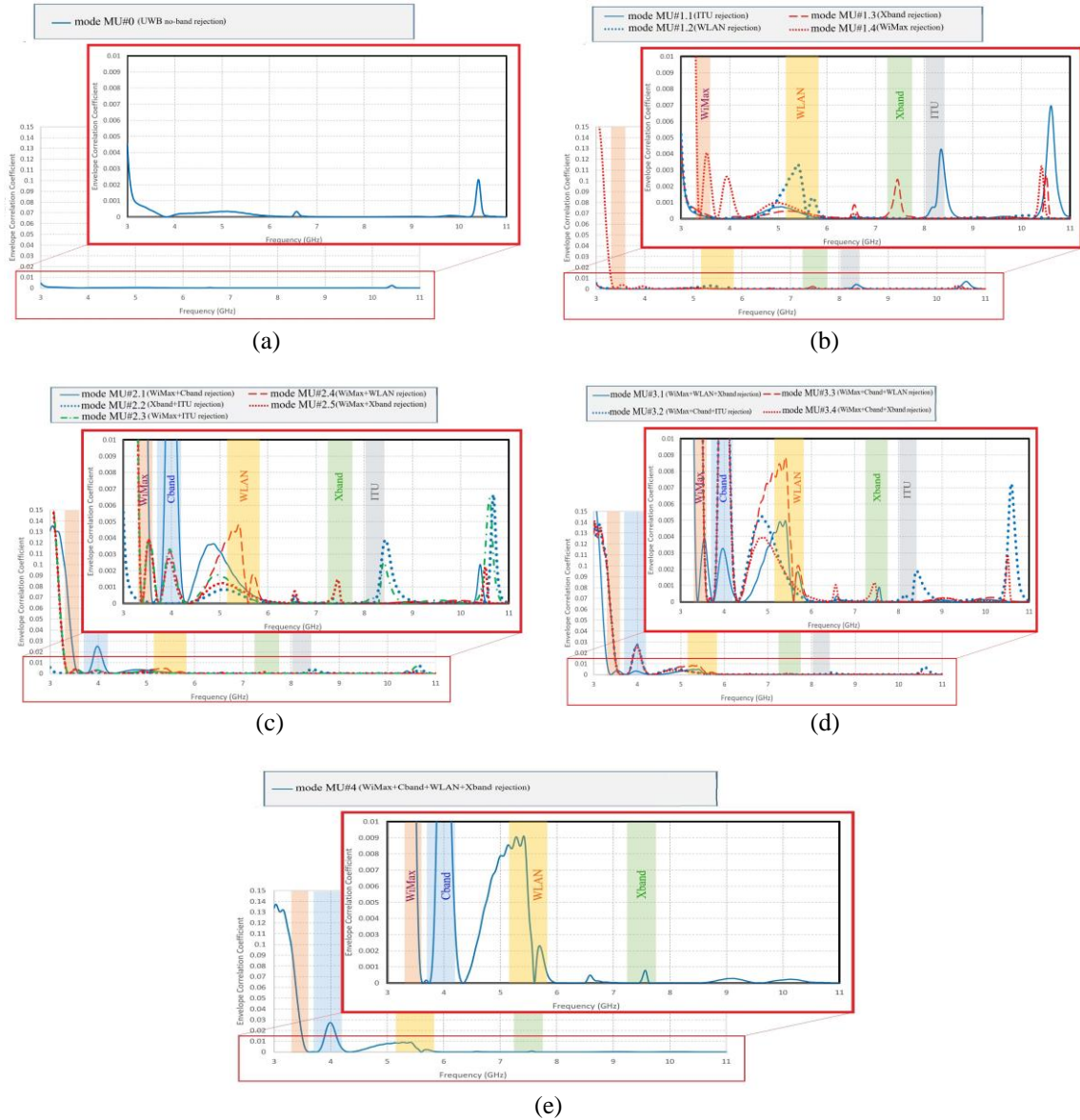


Figure 13. Envelope correlation coefficient of Ant#1 and Ant#2 at (a) UWB mode, (b) single-band rejection modes, (c) dual-band rejection modes, (d) triple-band rejection modes, and (e) quad-band rejection modes

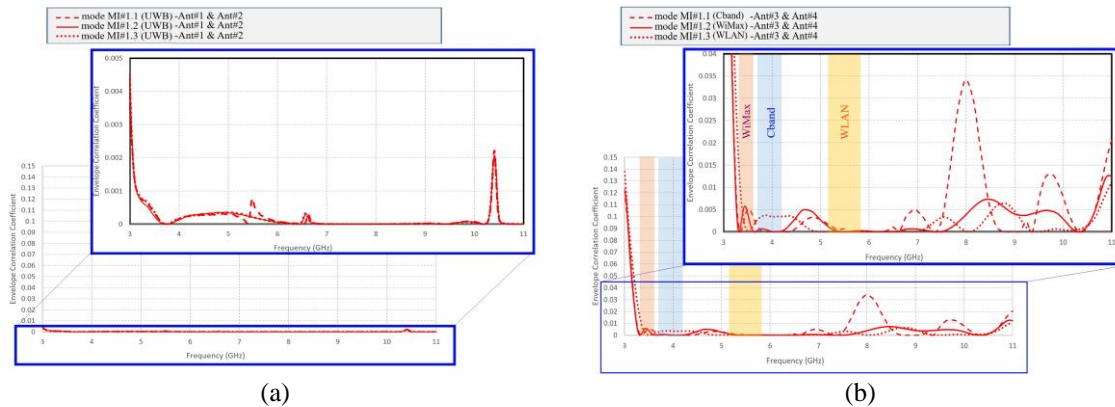


Figure 14. Envelope correlation coefficient in interweave modes of (a) Ant#1 and Ant#2 and (b) Ant#3 and Ant#4

3.6. Diversity gain

Diversity gain (DG) is an important factor to assess the performance of the MIMO antenna system. Good diversity characteristics are always indicated by DG values that are greater than 9 [20]. DG is so related to ECC and can be determined from the relation in (5) [21], [22].

$$DG = 10\sqrt{1 - |\rho_e|} \tag{5}$$

DG results in the underlay operating modes are displayed in Figure 15. Since ECC results approaching zero in this design it can be guessed to have excellent DG results that approaches 10. It can be seen that DG values of Ant#1 and Ant#2 are so close to 10 along the UWB range in mode MU#0 of Figure 15(a). Good diversity characteristics are also evidenced in all underlay modes where DG value ranges from 9.5 to 10 in the results of Figures 15(b) to 15(e). Moreover, Figure 16, which shows DG results in the interweave modes of operation shows that DG converges 10 between the sensing antennas as shown in Figure 16(a). Finally, good diversity is obtained between the communication antennas where DG value is greater than 9.7 in all cases of Figure 16(b).

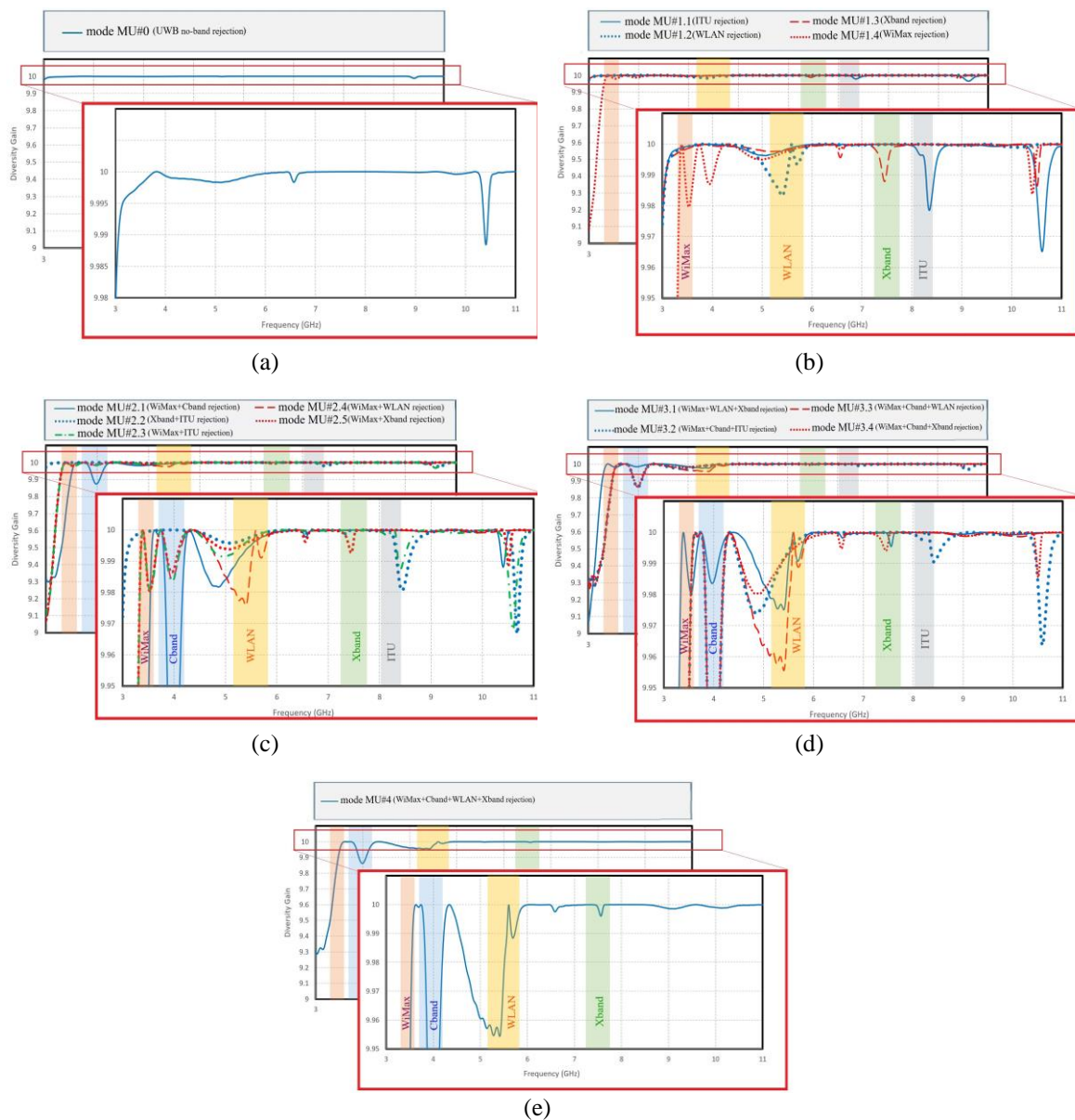


Figure 15. Diversity gain of Ant#1 and Ant#2 at (a) UWB mode, (b) single-band rejection modes, (c) dual-band rejection modes, (d) triple-band rejection modes, and (e) quad-band rejection modes

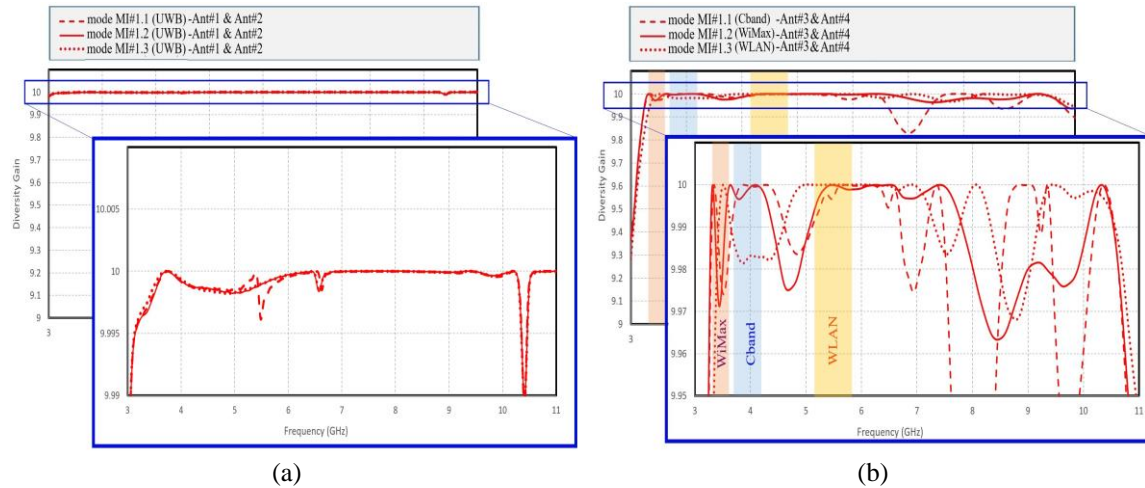


Figure 16. Diversity gain in interweave modes of (a) Ant#1 and Ant#2, and (b) Ant#3 and Ant#4

3.7. Comparison

This work is compared to recent MIMO CR designs as illustrated in Table 2. It is obvious that the design is novel where none of previous works gathers underlay and interweave CR in the same MIMO design. It can also be shown that the design is more suitable to serve CR whether in terms of number of MIMO operation modes or the flexibility it offers to select the notched or operation region. Comparison also shows that whilst this design offers whole UWB scanning a MIMO fashion, some of the works in Table 2 have only single scanning element.

Table 2. Comparison with recent MIMO cognitive radio designs

Ref.	Size (mm ³)	No. of Elem.	Diodes		CR	Op. mod.	MIMO Scan.	Scan.	Targeted bands	
			PIN	Var.					Rej.	Comm.
[6]	50×39.8×1.52	4	4	-	U	2	Yes	UWB	WLAN	-
[7]	64×36×1.95	2	4	-	U	4	Yes	UWB	WiMax, WLAN	-
[8]	30×14×0.8	2	2	-	U	2	Yes	UWB	WiMax	-
[23]	40×20×1.6	2	4	-	U	3	Yes	UWB	WiMax, WLAN	-
[24]	40×23×1.5	2	2	-	U	2	Yes	UWB	WLAN	-
[9]	80×80×1.6	4	-	2	I	8	Yes	2.35-5.9 GHz	-	2.6-3.6 GHz
[10]	120×60×1.5	2	6	2	I	7	Yes	1-4.5 GHz	-	0.9-2.6 GHz
[11]	120×60×1.56	3	-	2	I	7	No	0.75-7.65 GHz	-	1.75-2.48 GHz
[25]	60×40×1.6	3	-	4	I	11	No	2.2-7 GHz	-	2.3-6.3 GHz
[26]	200×150×1.5	8	-	4	I	6	Yes	1.4-4.85 GHz	-	1.4-2.2 GHz
[27]	120×60×1.56	5	-	4	I	7	No	0.75-7.65 GHz	-	1.77-2.51 GHz
Prop.	50×38×0.8	4	18	-	U/I	18	Yes	UWB	WiMax, Cband, WLAN, Xband, ITU	WiMax, Cband, WLAN

CR: cognitive radio, U: Underlay, I: Interweave

4. CONCLUSIONS

This paper presents a quad-port design that is novel as it acts both as an underlay and interweave MIMO CR system. System's ability to perform in scanning/band notching/ communication is basically validated based on the assessment of its outcomes. As a frequency reconfigurable MIMO system, this design shows ability to work in fourteen underlay modes, three interweave modes plus an UWB sensing mode. Band notching process successfully prohibiting one or more of the regions dedicated for WiMax, Cband, WiMax, Xband and ITU. On the other hand, the two communication antennas succeed to cover WiMax, Cband and WLAN in the three interweave modes. Results and comparison aspects all high rate this work as feasible MIMO system for CR applications.

ACKNOWLEDGEMENTS

The authors are highly grateful and thankful to Mustansiriya University, Al-Furat Al-Awsat Technical University and Al-Farabi University College for the support they provide to accomplish of this work.




REFERENCES

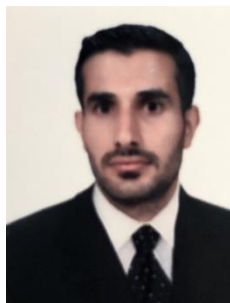
- [1] K. Patchala, Y. Raja Rao, and A. M. Prasad, "Triple band notch compact MIMO antenna with defected ground structure and split ring resonator for wideband applications," *Heliyon*, vol. 6, no. 1, p. e03078, Jan. 2020, doi: 10.1016/j.heliyon.2019.e03078.
- [2] R. Hussain, A. Raza, M. U. Khan, A. Shammim, and M. S. Sharawi, "Miniaturized frequency reconfigurable pentagonal MIMO slot antenna for interweave CR applications," *International Journal of RF and Microwave Computer-Aided Engineering*, vol. 29, no. 9, 2019, doi: 10.1002/mmce.21811.
- [3] Q. H. Kareem and M. J. Farhan, "Miniaturized quad-port UWB-MIMO antenna with band-notched characteristics at 5 GHz," *Progress In Electromagnetics Research C*, vol. 118, pp. 263–275, 2022, doi: 10.2528/PIERC22012002.
- [4] L. W. Abdullah, M. H. Wali, and A. H. Saloomi, "Twelfth mode on-demand band notch UWB antenna for underlay cognitive radio," *Indonesian Journal of Electrical Engineering and Computer Science (IJECS)*, vol. 22, no. 3, pp. 1446–1456, 2021, doi: 10.11591/ijeecs.v22.i3.pp1446-1456.
- [5] J. Costantine, Y. Tawk, S. E. Barbin, and C. G. Christodoulou, "Reconfigurable antennas: design and applications," *Proceedings of the IEEE*, vol. 103, no. 3, pp. 424–437, Mar. 2015, doi: 10.1109/JPROC.2015.2396000.
- [6] S. M. Khan, A. Iftikhar, S. M. Asif, A. D. Capobianco, and B. D. Braaten, "A compact four elements UWB MIMO antenna with on-demand WLAN rejection," *Microwave and Optical Technology Letters*, vol. 58, no. 2, pp. 270–276, 2016, doi: 10.1002/mop.29546.
- [7] A. Kholapure and R. G. Karandikar, "Printed MIMO antenna with reconfigurable single and dual band notched characteristics for cognitive radio," in *2017 IEEE International Conference on Antenna Innovations & Modern Technologies for Ground, Aircraft and Satellite Applications (iAIM)*, Nov. 2017, pp. 1–5, doi: 10.1109/IAIM.2017.8402566.
- [8] A. Quddus, R. Saleem, M. F. Shafique, and S. U. Rehman, "Compact electronically reconfigurable WiMAX band-notched ultra-wideband MIMO antenna," *Radioengineering*, vol. 27, no. 4, pp. 998–1005, 2018, doi: 10.13164/re.2018.0998.
- [9] T. Alam, S. R. Thummaluru, and R. K. Chaudhary, "Two-port MIMO wide-band antenna with two-port MIMO reconfigurable antenna for cognitive radio platforms," in *2018 IEEE Indian Conference on Antennas and Propagation (INCAP)*, Dec. 2018, pp. 1–4, doi: 10.1109/INCAP.2018.8770919.
- [10] X. Zhao, S. Riaz, and S. Geng, "A reconfigurable MIMO/UWB MIMO antenna for cognitive radio applications," *IEEE Access*, vol. 7, pp. 46739–46747, 2019, doi: 10.1109/ACCESS.2019.2909810.
- [11] R. Hussain and M. S. Sharawi, "Frequency reconfigurable MIMO slot and UWB sensing antennas for CR applications," in *2017 IEEE International Symposium on Antennas and Propagation & USNC/URSI National Radio Science Meeting*, Jul. 2017, vol. 2017-Janua, pp. 1693–1694, doi: 10.1109/APUSNCURSINRSM.2017.8072889.
- [12] J. Banerjee, A. Karmakar, R. Ghatak, and D. R. Poddar, "Compact CPW-fed UWB MIMO antenna with a novel modified Minkowski fractal defected ground structure (DGS) for high isolation and triple band-notch characteristic," *Journal of Electromagnetic Waves and Applications*, vol. 31, no. 15, pp. 1550–1565, Oct. 2017, doi: 10.1080/09205071.2017.1354727.
- [13] I. S. Masoodi, I. Ishteyaq, K. Muzaffar, and M. I. Magray, "A compact band-notched antenna with high isolation for UWB MIMO applications," *International Journal of Microwave and Wireless Technologies*, vol. 13, no. 6, pp. 634–640, Jul. 2021, doi: 10.1017/S1759078720001427.
- [14] L. W. Abdullah, A. H. Saloomi, and A. K. Jassim, "A single port frequency reconfigurable antenna for underlay/interweave cognitive radio," *Indonesian Journal of Electrical Engineering and Computer Science (IJECS)*, vol. 26, no. 2, pp. 859–868, May 2022, doi: 10.11591/ijeecs.v26.i2.pp859-868.
- [15] E. J. B. Rodrigues, H. W. C. Lins, and A. G. D'Assuncao, "Reconfigurable circular ring patch antenna for UWB and cognitive radio applications," in *8th European Conference on Antennas and Propagation (EuCAP 2014)*, 2014, pp. 2744–2748, doi: 10.1109/EuCAP.2014.6902393.
- [16] R. Hussain, M. S. Sharawi, and A. Shammim, "An integrated four-element slot-based MIMO and a UWB sensing antenna system for CR platforms," *IEEE Transactions on Antennas and Propagation*, vol. 66, no. 2, pp. 978–983, Feb. 2018, doi: 10.1109/TAP.2017.2781220.
- [17] H. Liu, G. Kang, and S. Jiang, "Compact dual band-notched UWB multiple-input multiple-output antenna for portable applications," *Microwave and Optical Technology Letters*, vol. 62, no. 3, pp. 1215–1221, Mar. 2020, doi: 10.1002/mop.31960.
- [18] L. Wu and Y. Xia, "Compact UWB-MIMO antenna with quad-band-notched characteristic," *International Journal of Microwave and Wireless Technologies*, vol. 9, no. 5, pp. 1147–1153, Jun. 2017, doi: 10.1017/S1759078716001239.
- [19] S. Riaz, X. Zhao, and S. Geng, "A compact frequency reconfigurable MIMO antenna with agile feedline for cognitive radio applications," in *10th International Conference on Communications, Circuits and Systems, ICCAS 2018*, Dec. 2018, pp. 176–179, doi: 10.1109/ICCCAS.2018.8769232.
- [20] L. Wajeeh Abdullah, Q. H. Kareem, M. Jasim Farhan, and A. Hasan Sallomi, "A dual port spatially diverse antenna system for cognitive radio applications," *Journal of Engineering and Sustainable Development*, vol. 24, no. Special, pp. 254–263, Aug. 2020, doi: 10.31272/jeasd.conf.1.28.
- [21] V. S. D. Rekha, P. Pardhasaradhi, B. T. P. Madhav, and Y. U. Devi, "Dual band notched orthogonal 4-Element MIMO antenna with Isolation for UWB Applications," *IEEE Access*, vol. 8, pp. 145871–145880, 2020, doi: 10.1109/ACCESS.2020.3015020.
- [22] V. N. K. R. Devana and A. M. Rao, "A novel dual band notched MIMO UWB antenna," *Progress in Electromagnetics Research Letters*, vol. 93, pp. 65–71, 2020, doi: 10.2528/pierl20080101.
- [23] R. Mathur and S. Dwari, "Compact planar reconfigurable UWB-MIMO antenna with on-demand worldwide interoperability for microwave access/wireless local area network rejection," *IET Microwaves, Antennas & Propagation*, vol. 13, no. 10, pp. 1684–1689, Aug. 2019, doi: 10.1049/iet-map.2018.6048.
- [24] A. Quddus, R. Saleem, and M. Bilal, "Reconfigurable band-notched UWB-MIMO antenna," in *2016 16th Mediterranean Microwave Symposium (MMS)*, Nov. 2016, pp. 1–4, doi: 10.1109/MMS.2016.7803839.
- [25] S.-P. Cheng and K.-H. Lin, "A reconfigurable monopole MIMO antenna with wideband sensing capability for cognitive radio using varactor diodes," in *2015 IEEE International Symposium on Antennas and Propagation & USNC/URSI National Radio Science Meeting*, Jul. 2015, pp. 2233–2234, doi: 10.1109/APS.2015.7305505.




- [26] R. Hussain, M. U. Khan, A. Kamran, and M. S. Sharawi, "Slot based frequency reconfigurable and UWB sensing MIMO antennas for CR applications," in *2019 IEEE International Symposium on Antennas and Propagation and USNC-URSI Radio Science Meeting*, Jul. 2019, pp. 907–908, doi: 10.1109/APUSNCURSINRSM.2019.8889247.

BIOGRAPHIES OF AUTHORS






Laith Wajeih Abdullah    is currently a part time Ph.D. student at the Department of Electrical Engineering, at Mustansiriyah University, Baghdad, Iraq. He is also an academic staff of the Communications Techniques Engineering Department at Al-Furat Al-Awsat Technical University, Najaf, Iraq. He received his B.Sc. degree in Electronics and Communication Engineering from the University of Baghdad, Baghdad, Iraq, in 1998 and his M.Sc. degree in 2002 from the University of Technology, Baghdad, Iraq. His research interests include reconfigurable antennas, cognitive radio, massive MIMO, wireless communications and IOT. He can be contacted at email: coj.lat@atu.edu.iq.



Qasim Hadi Kareem    received the B.S. degree in electrical engineering from Baghdad in 2012 and M.Sc. degree in electronics and communications engineering from the same university in 2015. He is working as lecturer in Computer Eng. Depart. in Al-Farabi University College from 2015. In 2022, he got Ph.D. Degree in communication Engineering from the department of electrical engineering at the University of Mustansiriyah in Baghdad. Currently performs work on MIMO wireless smartphone antennas with a polarized orthogonal function for potential 4G/5G smartphones as well as multi-band antennas and reconfigurable antennas. His research interests include wireless networking antennas. He can be contacted at email: qasim.hadi2017@gmail.com.



Adheed Hasan Sallomi    received the B.S. degrees in Electrical Engineering from Mosul University, Iraq, in 1982, and received M.S., and Ph.D. degrees in Electrical Engineering from University of Technology, Baghdad, Iraq, in 2000, and 2007 respectively. He is currently working at Electrical Engineering Department of Mustansiriyah University, Iraq. His research interests include radio waves propagation, channel modeling, smart antenna systems, and mobile communications. He has authored or co-authored over 30 scientific papers in the field of propagation, RF safety, and antennas. He can be contacted at email: adalameed@yahoo.com.